Available online at www.sciencedirect.com

ScienceDirect

Energy Procedia 97 (2016) 310 – 317

Energy Procedia

European Geosciences Union General Assembly 2016, EGU
Division Energy, Resources & Environment, ERE

Effect of Fluid Saturation on Gas Recovery from Class-3 Hydrate Accumulations Using Depressurization: A Case Study of the Yuan-An Ridge Site in Southwestern Offshore Taiwan

Yi-Jyun Huang, Cheng-Yueh Wu, Bieng-Zih Hsieh*

Department of Resources Engineering, National Cheng Kung University, Tainan City, Taiwan

Abstract

This study focused on the effect of initial hydrate saturation on gas recovery from a depressurized Class-3 hydrate accumulation via a simulation study of the Yuan-An Ridge hydrate deposit located in southwestern offshore Taiwan. Our simulation results showed that the recovery factors for a 20-year operation time in the case of a 70% pressure decline were 0.37, 0.47, 0.49, 0.51, and 0.13 for initial hydrate saturations of 30%, 40%, 50%, 60%, and 70%, respectively. The depressurization is not suitable for hydrate deposits with a high hydrate saturation over 70% except when the formation permeability is higher than 2 Darcy.

Peer-review under responsibility of the organizing committee of the General Assembly of the European Geosciences Union (EGU)

Keywords: Gas hydrate; Depressurization; Numerical simulation

1. Introduction

Gas hydrates (GHs) are crystalline compounds in which guest gas molecules are trapped in host lattices of ice crystals under high pressure and low temperature conditions. Generally, one mole of gas is encapsulated by five to seven moles of water. When the gas hydrates dissociate, there will be 150 ~ 180 unit volumes of gas and 0.8 unit

* Corresponding author. Tel.: +886-6-275-7575; fax: +886-6-238-0421.
E-mail address: bzhsieh@mail.ncku.edu.tw

Peer-review under responsibility of the organizing committee of the General Assembly of the European Geosciences Union (EGU)
doi:10.1016/j.egypro.2016.10.006

volumes of water released [1].

Gas hydrates can be found in permafrost, deep marine sediments, and seabeds. The global resources of gas hydrates are estimated to be at least twice those of conventional fossil fuels [2]. Gas hydrates could serve as a clean energy source for the next generation because the combustion of the natural gas from hydrate dissociation produces lower greenhouse gas emissions than conventional fossil fuels.

Gas hydrate deposits can be divided into three major classes [3]. Class-1 GH deposits are a hydrate-bearing layer (HBL) accompanied by an underlying free gas zone. Class-2 GH deposits are a HBL accompanied by an underlying mobile water zone. Class-3 GH deposits are an isolated hydrate layer without an underlying zone of mobile fluids; the entire hydrate layer can be well within the hydrate stability zone covered by impermeable upper- and lower-burden rocks. The bottom of GH deposits can be recognized by the signals from a bottom simulating reflector (BSR), which occur because of a negative acoustic impedance contrast (i.e. higher acoustic impedance above and lower acoustic impedance below) when analyzing seismic data.

A disturbance to the phase stability of the gas hydrate can release natural gas from it. Gas hydrates exist in a high-pressure low-temperature environment, so depressurization and thermal stimulation are both useful methods to make gas hydrates dissociate. Depressurization creates a low-pressure environment, which is unfavorable for GH solid phase stability and triggers GH dissociation. Thermal stimulation uses heat to dissolve the gas hydrate and release natural gas. However, heat loss and energy consumption are issues for the thermal stimulation method as well as the extension of efficient heating zone. Therefore, depressurization is regarded as a more effective method to produce natural gas from the hydrate deposits.

The assessment of gas production performance and the observation of GH productivity from depressurization can be studied by numerical simulation. Moridis et al. [4] used TOUGH+ to simulate gas production of a Class-3 GH reservoir located in the Tigershark area by depressurization and thermal methods. The results demonstrated that depressurization leads to better performance than the thermal method. Zhou et al. [5] studied the Nankai Trough in Japan by using a simulator. Geomechanics issues in the depressurization method were studied with the simulator. Konno et al. [6] investigated gas production performance and key factors for Class-3 GH deposits in the Eastern Nankai Trough and the Gulf of Mexico by simulation (MH21-HYDRES). Su et al. [7] used TOUGH+ to investigate the potential of the site SH-3 in the Shenghu area of China.

For the depressurization method, the dissociation efficiency is controlled by the response of the hydrate to the propagating pressure disturbance. The pressure propagation is related to the fluid effective permeability, which is a function of the amount (or saturation) of the mobile fluid in the pore spaces of the hydrate layer. Therefore, the effect of initial hydrate saturation on the production performance should be studied. The purpose of this study was to investigate the effect of initial hydrate saturation on gas recovery from a depressurized Class-3 hydrate deposit. A simulation study of the Yuan-An Ridge hydrate deposit located in southwest offshore Taiwan was performed.

2. Geological setting

Significant efforts to evaluate the reserves of hydrates in Taiwan have begun recently. BSR investigations have identified large gas hydrate resources in southwestern offshore Taiwan. Because of the extremely low energy independence ratio (below 5%) of Taiwan, offshore gas hydrate resources could serve as an opportunity to improve the energy independence of Taiwan.

The Yuan-An Ridge hydrate deposit located in southwest offshore Taiwan was studied in this research (Fig. 1). The Yuan-An Ridge hydrate deposit was found through a BSR [8]. The studied site is a ridge-type gas hydrate deposit with a variable net-thickness measuring from 0.45 to 66.93 m. The investigated area is 2.56 km^2. Based on a geophysical investigation, the formation porosity is about 0.16 and the permeability is about 1 Darcy (1,000 mD). The best guess of the initial gas hydrate saturation is about 50% according to the seismic survey and the BSR analysis [9]. This reservoir is assumed to be a Class-3 GH deposit with two phases of hydrate and water. The formation pressure and temperature at the depth of the BSR (1520 m) were measured as 16.4 MPa and 17.2°C, respectively.

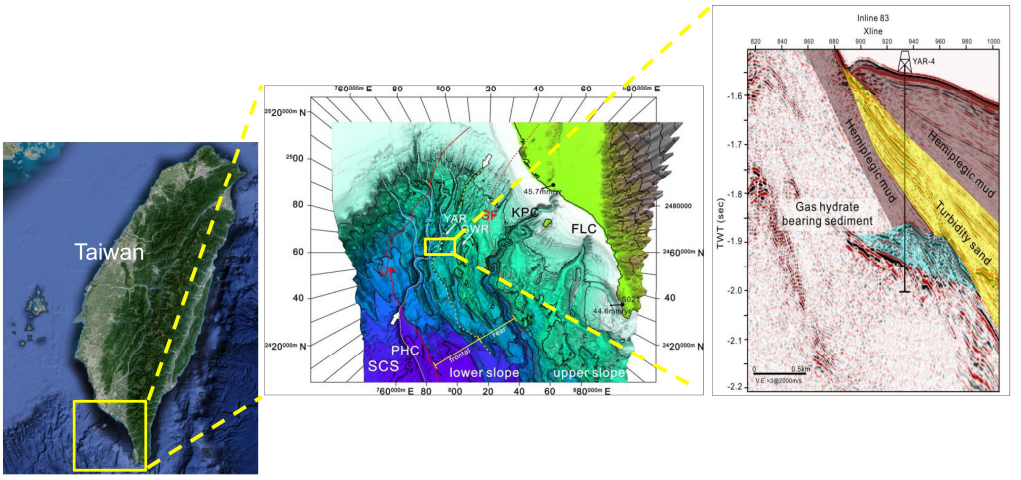

Fig. 1. Location and discovery of Yuan-An Ridge (YAR) hydrate deposit [8,9].

3. Study method

Numerical simulation was used in this research to study the dissociation of hydrates and the production of gas from a Class-3 GH deposit. The simulator we used was the STARS simulator developed by the Computer Modelling Group Ltd. (CMG). The STARS simulator is a comprehensive steam-thermal-advanced processes reservoir simulator that couples the heat transfer, geo-chemical, geo-mechanical, and multiphase fluid flow mechanisms. The calculation performance of the STARS simulator for gas hydrate production was validated via code comparison supported by the National Energy Technology Laboratory [10].

4. Simulation model construction

The first step for the simulation model construction is to build a geological model from the collected formation surface and bottom structural maps and the closure area map. The pre-processing simulator BUILDER was used to build the geological model by dividing the Yuan-An Ridge structure into grids and defining the formation parameters in each grid block, including the porosity, permeability, and the assumed rock compressibility.

The pressure-volume-temperature (PVT) data, rock-fluid properties (relative permeability and capillary pressure curves), and formation initial conditions (initial formation pressure, temperature, and hydrate saturation) were then assigned sequentially to each grid block. The relative permeability curve model we used was based on the Stone and Aziz model [11,12] with an irreducible water saturation of 0.2, irreducible gas saturation of 0.1, and an exponent (*n*-value) of 4. The capillary pressure curves were derived from the Van-Genuchten equation [13]. Different values of the initial hydrate saturation ranging from 0.3 to 0.7 were considered in this case study; an initial hydrate saturation of 0.5 was used in the base case.

Next, the completion (well location and perforation intervals) and operating conditions (pressure drops and production rate constraints) were designed, completing the simulation model. A 1 km long horizontal well was placed at the updip of the structure, and constant-pressure depressurization was designed as the operating condition with a 20-year usable life. Different scenarios for constant-pressure operation were considered in this case study. The degrees of pressure decline studied were 70%, 60%, 50%, and 40% from the initial formation pressure.

5. Results

The base case of the depressurization used a constant bottom-hole pressure of 5 MPa (i.e. 70% bottom-hole pressure drop from the initial formation pressure, Δp = 70%) at the hydrate deposit with an initial hydrate saturation of 0.5 (S_h = 0.5). The changes in reservoir pressure, temperature, and saturation due to hydrate dissociation and fluid production were calculated. Fig. 2 shows the production profiles of gas and water, cumulative gas production, and cumulative water production as they change with time.

During the early stage of depressurization, mobile water was produced first (Fig. 2). The production of water was a key to lowering the reservoir pressure in order to create a low-pressure environment for the hydrate dissociation. After the hydrate dissociated and the saturation of released gas in the formation was higher than the critical saturation (S_{girr} = 0.1), the gas moved toward the well and produced at the surface. A three-peak gas production profile was observed from this case (Fig. 2). The gas production peaks were related to the boundary effect, since the pressure front touched the left (west), right (east), and south boundaries sequentially. After 4 years of production, the simulated average reservoir pressure declined about 70%, making the pressure differential between the wellbore and the formation pressures become zero, which in turn caused gas production to cease. The cumulative gas production was 511 MMSCM and the recovery factor (RF) was 0.49 for this base case (Fig. 2).

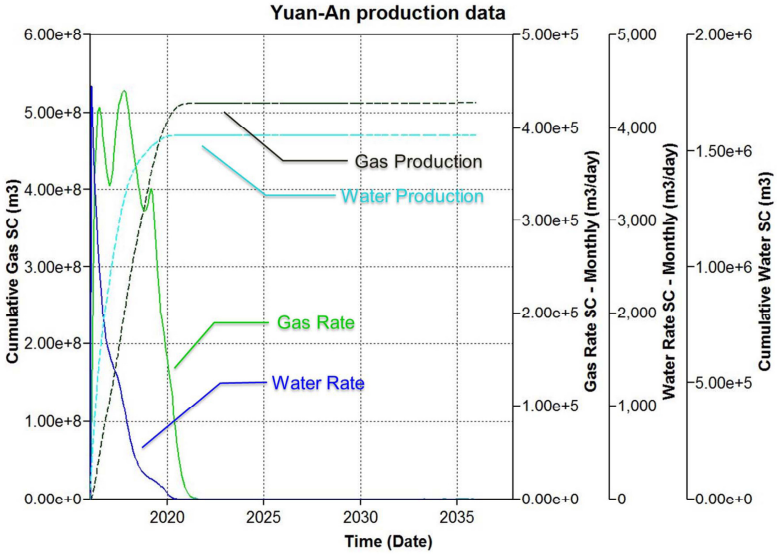

Fig. 2. Production profiles of gas and water and cumulative gas and water productions for the base case of Δp = 70% and S_h = 0.5.

After the base case study, the effect of the initial hydrate saturation (S_h) on the recovery factor (RF) was studied. The initial hydrate saturation was assumed to range from 0.3 to 0.7.

The change of cumulative gas production with time for different initial hydrate saturations (S_h = 0.3, 0.4, 0.5, 0.6 and 0.7) was calculated (Fig. 3). When the initial hydrate saturation (S_h) was 0.7, the reservoir pressure did not readily decline due to the small amount of mobile water, and a low gas production rate was obtained for the whole production period (20 years) (Fig. 3).

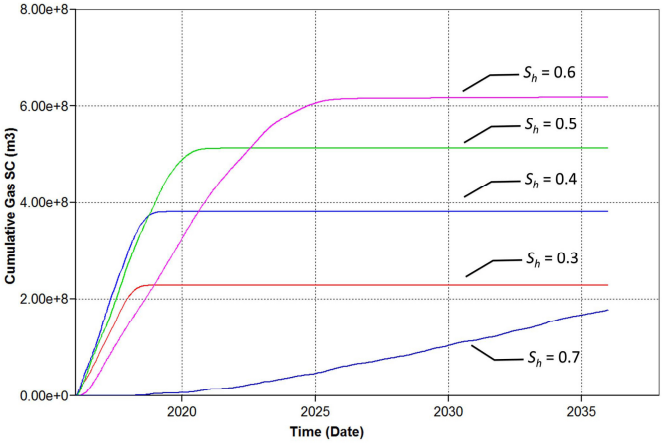

Fig. 3. Cumulative gas production over time for different initial hydrate saturations (S_h = 0.3, 0.4, 0.5, 0.6 and 0.7) and Δp = 70%.

The recovery factor (RF) for each case was calculated. Fig. 4 shows the recovery factor changing with the initial hydrate saturation (S_h) for the depressurization case of Δp = 70%. The best recovery factor was observed when the initial hydrate saturation was 0.6. The lowest recovery factor was found with an initial hydrate saturation of 0.7. The low recovery factor for the case of S_h = 0.7 was due to the low initial water saturation with a low effective permeability to water; consequently the degree of reservoir pressure decline was limited.

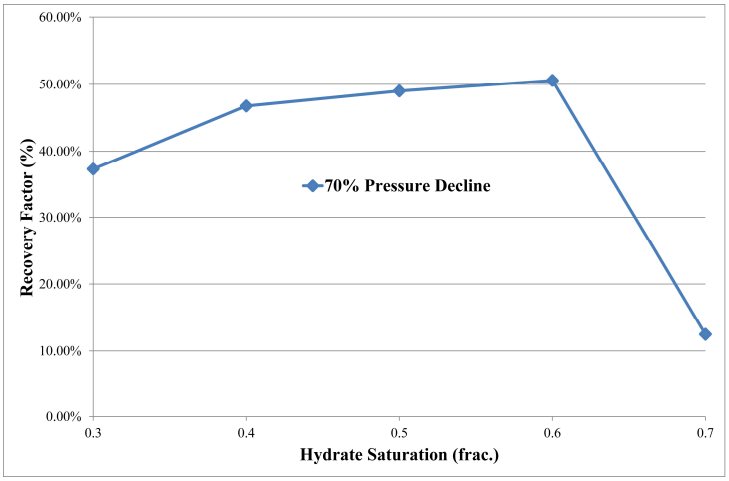

Fig. 4. Recovery factor (RF) vs. initial hydrate saturation (S_h) for the case of Δp = 70%.

6. Discussions

A sensitivity analysis was performed with respect to the impact of the wellbore pressure drop, well placement, formation permeability, and fluid relative permeability on the recovery factor (RF) for different initial hydrate saturations (ranging from 0.3 to 0.7).

6.1. Wellbore pressure drop

The degree of wellbore pressure drop was a very sensitive parameter for the RF of a Class-3 hydrate deposit in

every case of the initial hydrate saturation. Based on the simulation results (Fig. 5), it was not easy to produce gas in a Class-3 hydrate deposit when the wellbore pressure drop was less than 40%. In this case study, a wellbore pressure drop of 50% had just over 0.1 RF in the case of S_h = 0.5. This is the optimal result compared to the other cases of initial hydrate saturation (Fig. 5). When a wellbore pressure drop of over 60% was used, the hydrate deposit with an initial hydrate saturation of 0.6 (S_h =0.6) always had the best recovery factor. The larger the wellbore pressure drop, the higher the recovery factor. The threshold wellbore pressure drop of a Class-3 hydrate deposit using depressurization was 40%. However, a large wellbore pressure drop still cannot help to raise the RF of Class-3 hydrate deposits with an initial saturation over 0.7 ($S_h \geq 0.7$).

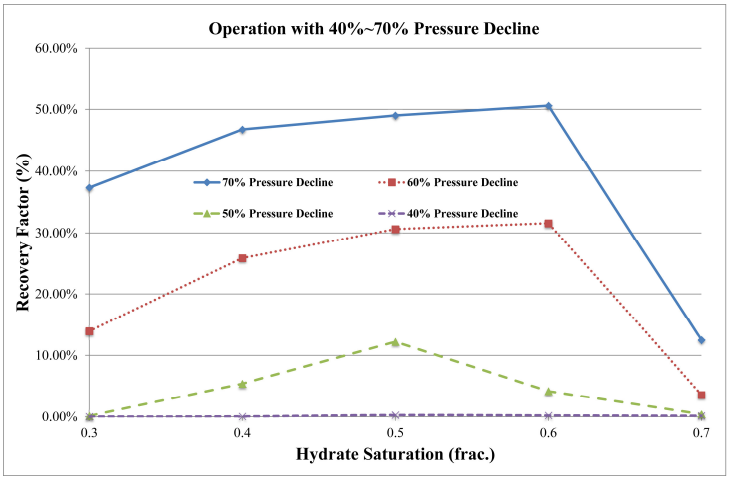

Fig. 5. Effect of wellbore pressure drop on RF for initial hydrate saturations of 0.3, 0.4, 0.5, 0.6, and 0.7.

6.2. Well placement

This test was to investigate the effect of the well placement layer on the RF of a Class-3 hydrate deposit in every case of the initial hydrate saturation. This study divided the formation into 5 layers and placed the horizontal well in the top layer in the base case. Since the dissociated gas tends to migrate upward due to the gravity difference, a higher recovery factor can be expected when the well is placed in the top layer (Fig. 6). The lower the well placement in a formation, the lower the recovery factor. However, the influence of the well placement layer on the RF of a Class-3 hydrate deposit is less than 5%. The influence of well placement layer on the RF of a high-saturation ($S_h \geq 0.7$) hydrate deposit can be ignored (Fig. 6).

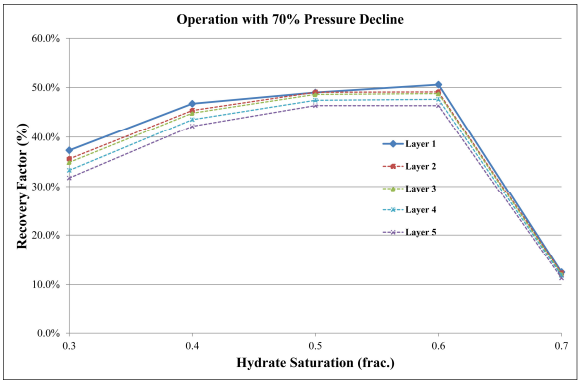

Fig. 6. Effect of well placement layer on RF for initial hydrate saturations of 0.3, 0.4, 0.5, 0.6, and 0.7.

6.3. Formation permeability

Formation permeabilities of 100, 500, 1000, 2000, and 10000 mD were considered in this sensitivity test to study their effect on the RF of a Class-3 hydrate deposit with different initial hydrate saturations.

Basically, a formation permeability threshold of 500 mD allows two groups to be observed (Fig. 7). The low formation permeability environment was not favorable to the production of Class-3 hydrate deposits with initial hydrate saturation (S_h) over 0.5, especially when the formation permeability value was less than 500 mD (Fig. 7). When the formation permeability was higher than 500 mD (the second group), the RF of a Class-3 hydrate deposit is not affected by the formation permeability if the initial hydrate saturation is less than 0.6 ($S_h \leq 0.6$) (Fig. 7). The formation permeability had the most influence when $S_h \geq 0.7$. This test showed the development probability for a Class-3 hydrate deposit with high initial hydrate saturation ($S_h \geq 0.7$) relies on a very high formation permeability ($k \geq 2$ Darcy).

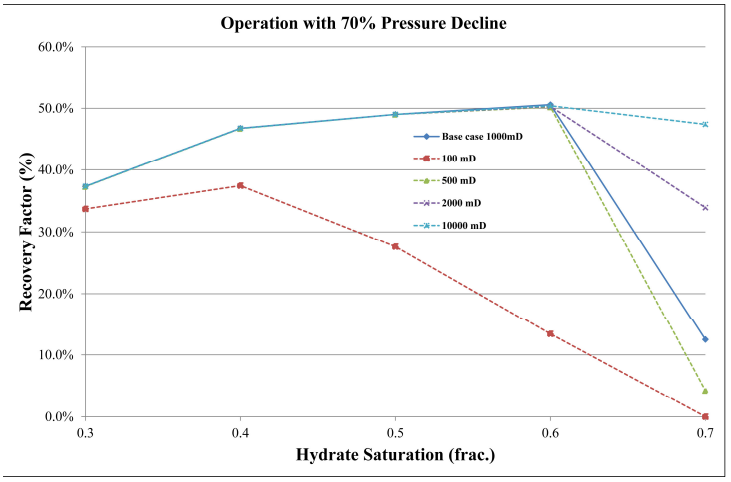

Fig. 7. Effect of formation permeability on RF for initial hydrate saturations of 0.3, 0.4, 0.5, 0.6, and 0.7.

6.4. Relative permeability

To study the effect of relative permeability on the RF of a Class-3 hydrate deposit, the *n*-value, which is used to control the curvature of the relative permeability of gas and water in the Stone and Aziz method, was varied. The chosen *n*-values were 4 (base case), 3 and 1. The relative permeability curve became more linear as the *n*-value changed from 4 to 1. A linear-type relative permeability has a higher fluid mobility.

The test results (Fig. 8) showed that the RF of a Class-3 hydrate deposit is not affected by the *n*-value when the initial hydrate saturation is less than 0.6 ($S_h \leq 0.6$). The *n*-value had the most influence on the high initial hydrate saturation cases of $S_h \geq 0.7$. This test showed that the development for a Class-3 hydrate deposit with a high initial hydrate saturation ($S_h \geq 0.7$) can be considered when a favorable *n*-value (*n*-value ≤ 3) exists in a high initial hydrate saturation deposit with a high formation permeability ($k \geq 1$ Darcy).

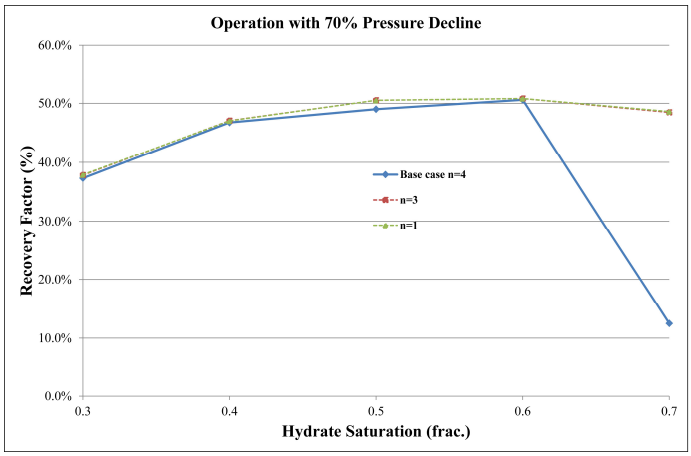

Fig. 8. Effect of relative permeability on RF for initial hydrate saturations of 0.3, 0.4, 0.5, 0.6, and 0.7.

7. Conclusions

1. Gas recovery changes with different initial hydrate saturations. A Class-3 hydrate deposit with an initial hydrate saturation of 60% has the highest recovery factor. This can be useful information for GH site screening.
2. The case study showed that a recovery factor of 0.5 can be obtained when a depressurization pressure drop of 70% is used on the Yuan-An Ridge hydrate deposit with an initial hydrate saturation of 60%.
3. We found that the depressurization operation is not suitable for Class-3 hydrate deposits with extremely high hydrate saturation of above 70% and the formation permeability less than 1 Darcy.

Acknowledgements

This work was supported by grant MOST 105-3113-M-002-006 from the Ministry of Science and Technology (MOST), Taiwan. The authors specially thank to Dr. Andrew T.S. Lin and his research team members to provide the geological and geophysical information of Yuan-An Ridge hydrate deposit.

References

[1] Byk SSh, Formina VI. Gas hydrates. Russian Chemical Reviews 1968; 37:340-352.
[2] Sloan ED, Koh CA. Clathrate hydrates of natural gases. 3rd. New York: Marcel Dekker; 2007.
[3] Moridis GJ, Collett TS. Strategies for gas production from hydrate accumulations under various geologic conditions. Lawrence Berkeley National Laboratory 2003; LBNL-52568.
[4] Moridis GJ, Matthew TR. Strategies for gas production from oceanic class 3 hydrate accumulations. Offshore Technology Conference, Houston, 2007.
[5] Zhou ML, Soga K, Xu E, Uchida S, Yamamoto K. Numerical study on Eastern Nankai Trough gas hydrate production test. Offshore Technology Conference, Houston, 2014.
[6] Konno Y, Masuda Y, Hariguchi Y, Kurihara M, Ouchi H. Key factors for depressurization-induced gas production from oceanic methane hydrates. Energ Fuel 2010; 24:1736-1744.
[7] Su Z, He Y, Wu N, Zhang K, Moridis GJ. Evaluation on gas production potential from laminar hydrate deposits in shenhu area of South China Sea through depressurization using vertical wells. J Petrol Sci Eng 2012; p. 87–98.
[8] Li KS, Lin TS. Three-Dimensional structural and stratigraphic architectures and gas hydrate occurrences in a fault zone of the accretionary wedge Off SW Taiwan. 12th International Conference on Gas in Marine Sediment, Taipei, 2014.
[9] Lin CC. Geological controls of gas hydrate occurrences and gas hydrate resource assessment, offshore southwest Taiwan. Taipei: National Central University; 2013.
[10] Gaddipati M. Code comparison of methane hydrate reservoir simulators using CMG STAR. West Virginia: West Virginia University; 2008.
[11] Aziz K, Settari A. Petroleum reservoir simulation. Applied Science Publishers 1979.
[12] Stone HL. Probability model for estimating three-phase relative permeability. J Pet Tech 1970;22:214-218.
[13] Van Genuchten MT. A Closed-form equation for predicting the hydraulic conductivity of unsaturated soils. Soil Sci Soc Am J 1980; 44:892-898.